Frontiers of Information Technology & Electronic Engineering
www.zju.edu.cn/jzus; engineering.cae.cn; www.springerlink.com
ISSN 2095-9184 (print); ISSN 2095-9230 (online)
E-mail: jzus@zju.edu.cn

Capacity analysis for cognitive heterogeneous networks with ideal/non-ideal sensing*

Tao HUANG, Ying-lei TENG, Meng-ting LIU, Jiang LIU†‡
(*State Key Laboratory of Networking and Switching Technology*, *Beijing University of Posts and Telecommunications*, *Beijing 100876*, *China*)
†E-mail: liujiang@bupt.edu.cn

Received Apr. 10, 2014; Revision accepted Oct. 28, 2014; Crosschecked Dec. 12, 2014

Abstract: Due to irregular deployment of small base stations (SBSs), the interference in cognitive heterogeneous networks (CHNs) becomes even more complex; in particular, the uncertainty of spectrum mobility aggravates the interference context. In this case, how to analyze system capacity to obtain a closed-form expression becomes a crucial problem. In this paper we employ stochastic methods to formulate the capacity of CHNs and achieve a closed-form expression. By using discrete-time Markov chains (DTMCs), the spectrum mobility with respect to the arrival and departure of macro base station (MBS) users is modeled. Then an integral method is proposed to derive the interference based on stochastic geometry (SG). Also, the effect of sensing accuracy on network capacity is discussed by concerning false-alarm and miss-detection events. Simulation results are illustrated to show that the proposed capacity analysis method for CHNs can approximate the conventional sum methods without rigorous requirement for channel station information (CSI). Therefore, it turns out to be a feasible and efficient way to capture the network capacity in CHNs.

Key words: Cognitive heterogeneous networks, Markov chain, Stochastic geometry, Homogeneous Poisson point process (HPPP)
doi:10.1631/FITEE.1400129 **Document code:** A **CLC number:** TP393

1 Introduction

With the wireless data requirements increasing rapidly nowadays, small-cell networks (Bennis *et al.*, 2013; Hwang *et al.*, 2013; Nakamura *et al.*, 2013; Fehske *et al.*, 2014) have been viewed as an important complement for the regular hexagon cellular networks, which can provide high-throughput gains for both indoor and outdoor hotspots. Although many advantages can be obtained by introducing small cell networks, the interference including cross-tier interference and co-tier interference becomes even more severe in heterogeneous networks, which can severely degrade the performance of networks.

Fortunately, cognitive radio brings tremendous spectrum usage, which is able to solve the spectrum usage and interference management. Therefore, introducing cognition into small cells through spectrum sensing has attracted a lot of attention. It can be used to avoid severe interference to/from macro base stations (MBSs) and enhance the total network performance (Akoum *et al.*, 2010; ElSawy and Hossian, 2013). However, to what extent can the capability of heterogeneous networks be improved? To the best of our knowledge, the results presented in the literature are far from perfect in handling this question. In fact, there are rare ones that can provide the closed-form network capacity expression for cognitive heterogeneous networks (CHNs) because of the interference and complicated network association, especially when spectrum mobility is involved in performance analysis.

‡ Corresponding author
* Project supported by the National Basic Research Program (973) of China (No. 2012CB315801), the National Natural Science Foundation of China (Nos. 61302089 and 61302081), and the State Major Science and Technology Special Projects (No. 2013ZX03001025-002)
ORCID: Jiang LIU, http://orcid.org/0000-0002-0729-1299

Recently, there has been a tendency of using stochastic geometry (SG) theory to capture the topological distribution of the infrastructure in multi-tier cellular networks. For the SG theory, some interesting conclusions have been drawn. Andrews *et al.* (2011) have verified that the Poisson point process (PPP) serves better in capturing the increasingly opportunistic and dense placement of base stations in future networks. Also, PPP has been proved a useful tool to model co-channel interference from MBSs or small base stations (SBSs) (Akoum *et al.*, 2011; Madhusudhanan *et al.*, 2012). Dhillon *et al.* (2012a) studied the *K*-tier downlink heterogeneous cellular network model under the assumption of PPP for each tier. The results show that adding more tiers and/or base stations (BSs) neither increases nor decreases the probability of coverage or outage when all the interference-limited tiers have the same target signal-to-interference-plus-noise ratio (SINR). Heath *et al.* (2013) used the Gamma distribution with second-order moment matching to model co-tier and cross-tier interference distributions. The results showed that the calculation of the success probability and average rate can be simplified, incorporating small- and large-scale fading.

Some researchers also attempted to use the SG model in CHNs (Khoshkholgh *et al.*, 2013; ElSawy *et al.*, 2013a; 2013b). ElSawy *et al.* (2013a) used SG to model and analyze heterogeneous cellular networks. They first exploited SG to evaluate the load of each network tier, and then obtained the maximal frequency reuse efficiency with spectrum sensing design for channel access with the assumption of a hard core point process (HCPP). Khoshkholgh *et al.* (2013) gave a performance analysis for two-tier heterogeneous networks (HetNets) with cognitive small cells under the SG model with respect to the outage probability. They obtained the opportunistic spectrum access probability for small-cell access points conditioned by the spectrum sensing threshold. ElSawy *et al.* (2013b) summarized the previous work related to SG in the literature for single-tier, multi-tier, as well as cognitive cellular wireless networks. They pointed out that only a few results in the context of multi-tier cellular networks are available to CHNs and indicated that there are opportunities for innovating techniques which facilitate SG modeling. Although some work has been done to try to figure out capacity analysis for CHNs, the closed-form network capacity expression was not well considered. ElSawy *et al.* (2013a) focused only on the performance of cognitive small-cell networks and the outage probability for a small-cell user. Khoshkholgh *et al.* (2013) achieved a closed-form expression for the outage performance in a Rayleigh fading environment through Laplace transform. However, the work was elaborated in the underlay fashion where the outage event for primary users (PUs) is caused mainly by the aggregated interference from secondary users (SUs) and the noise environment. In addition, the closed-form derivation of interference from SUs to PU was obtained only in the large-scale environment.

Moreover, from the analysis mentioned above, we can clarify some facts and difficulties in obtaining capacity derivation for cognitive multi-tier cellular networks: (1) The objective of CHNs is different from that of conventional cognitive radio networks (CRNs) (i.e., cognitive networks with licensed and unlicensed users). That is, we need to focus on capacity aggregation for both MBSs (similar to PUs in conventional CRNs) and cognitive SBSs (similar to SUs in conventional CRNs) rather than an opportunistic utilization of SUs on the unlicensed band, subject to a tolerable performance degradation for the PUs. (2) Spectrum access is sensitive to its mobility model, which affects capacity derivation significantly. (3) The calculation of interference becomes even more difficult in CHNs. For one thing, the small-cell infrastructure confuses traditional regular deployment and the spectrum reuse policy, and the interference becomes complicated to observe. For the other, it is never too easy to obtain channel station information (CSI) in the multi-cell system, especially in multi-tier networks.

Therefore, different from previous studies, a closed-form expression for the capacity of CHNs is proposed based on the SG theory in this paper. We employ the divide-and-conquer strategy, deriving the spectrum usage opportunity by discrete-time Markov chains (DTMCs), and managing to approximate the aggregated interference by an integral method, which takes the integral of the probability of the interference according to the stochastic distribution of distance between nodes. By simulation under the homogeneous Poisson point process (HPPP), we are able to show that the proposed approach achieves a better

approximation to the conventional aggregation interference method which depends on the precise measure of CSI, which is an obstacle in CHNs. Also, we derive the impact of sensing results by modifying factors in the Markov chain and make comparison with ideal/non-ideal sensing.

2 System model

In this paper we focus on a downlink two-tier CHN where MBSs and SBSs are located in a circular coverage with radius R. All the users associate with the BSs, which provide the highest reference signal receiving power (RSRP). Meanwhile, we assume that MBSs and their users use the licensed spectrum band, while SBSs and their users act as the unlicensed users that access the idle channels. Therefore, they work in an overlay manner similar to a typical cognitive radio system; i.e., MBSs and their users work as PUs, and SBSs and their users are SUs. Note that both of them serve as the cellular network. Thus, both the capacities of MBSs and SBSs need to be taken into consideration in CHNs. Each time slot is divided into two periods, i.e., sensing period T_s (where SBSs and their users scan throughout the spectrum band) and data transmission period (where SBSs access the channel if finding a vacancy for MBSs). The structure of the frame is illustrated in Fig. 1. The time for merging the sensing results and their feedback to the serving SBSs is ignored. Here we assume that at most one user is allowed to access the channel during the time slot for each macro cell or small cell, while the same frequency can be reused in other cells.

Instead of assuming MBSs and SBSs are placed deterministically in a grid model, we adopt an HPPP model in this paper, where MBSs and SBSs follow the HPPP process with density λ_M and λ_F, respectively. Also, users located in the CHNs follow the HPPP with density λ_U, which includes X MBS users and Y SBS users. The idea of HPPP derives from SG which aims at averaging over all the network topologies seen from a generic node weighted by their probability of occurrence. HPPP has been shown by Dhillon *et al.* (2012b) as an equally accurate model to capture the performance of the network compared with the conventional grid model, whereas the former is more preferable for its tractability and better at describing the increasing opportunistically placed base stations in the future.

In the context of two-tier CHNs, there exist two kinds of interference (Fig. 1), i.e., co-tier and cross-tier interference. Specifically, for the MBS users, co-tier interference comes from other MBSs while cross-tier interference is caused by all the SBSs. Likewise, for the SBS users, co-tier interference derives from other SBSs while signals from all MBSs lead to cross-tier interference. We assume that all MBSs and SBSs simultaneously transmit to their associated users with the same power P_M and P_F,

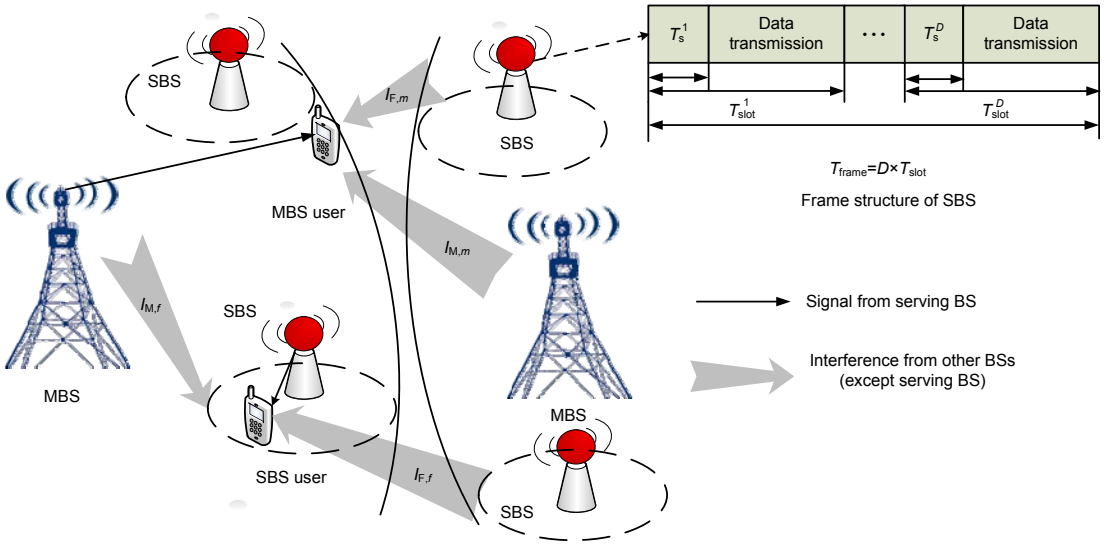

Fig. 1 Illustration of a two-tier heterogeneous network

respectively. Let g_{M} denote the transmission gain from MBS to its serving user. Similarly, g_{F} is the transmission gain from SBS to its serving user. The noise is assumed to be a zero-mean complex additive white Gaussian random variable with power P_{Noise}.

Generally speaking, the sensing results of SBSs greatly impact the interference context. Therefore, we discuss the SINR of both MBSs and SBSs from the aspect of variant sensing results, i.e., ideal sensing with no sensing error and non-ideal sensing with miss-detection or false-alarm events.

For the case of ideal sensing, there is no interference between two tiers, and thus only co-tier interference exists. The SINRs of MBS and SBS users are

$$\mathrm{SINR}_m=\frac{P_{\mathrm{M}}g_{\mathrm{M}}}{I_{\mathrm{M},m}+P_{\mathrm{Noise}}}, \tag{1}$$

$$\mathrm{SINR}_f=\frac{P_{\mathrm{F}}g_{\mathrm{F}}}{I_{\mathrm{F},f}+P_{\mathrm{Noise}}}, \tag{2}$$

where $I_{\mathrm{M},m}$ is the interference for MBS user m from other MBSs, and $I_{\mathrm{F},f}$ is the interference caused by other SBSs for SBS user f.

For the case of non-ideal sensing, the events of miss-detection and false-alarm would cause cross-tier interference for both MBSs and SBSs. Accordingly, for MBS and SBS users, their SINRs are

$$\overline{\mathrm{SINR}}_m=\frac{P_{\mathrm{M}}g_{\mathrm{M}}}{I_{\mathrm{M},m}+I_{\mathrm{F},m}+P_{\mathrm{Noise}}}, \tag{3}$$

$$\overline{\mathrm{SINR}}_f=\frac{P_{\mathrm{F}}g_{\mathrm{F}}}{I_{\mathrm{M},f}+I_{\mathrm{F},f}+P_{\mathrm{Noise}}}, \tag{4}$$

where $I_{\mathrm{F},m}$ stands for the interference from all the SBSs to MBS user m, and $I_{\mathrm{M},f}$ is the interference caused by all the MBSs to SBS user f.

3 Capacity derivation for cognitive heterogeneous networks

In the CHN model, it is hard to derive the capacity due to the uncertainty of spectrum mobility and the complex interference between users and heterogeneous base stations. As DTMC has advantages in analyzing the reliability and performance of the service portfolio (Gelabert *et al.*, 2010; Huang *et al.*, 2011; Meerja *et al.*, 2011), we consult the Markov chain to derive the distribution of time slots under different sensing results; meanwhile, the interference is captured with the HPPP assumption in an SG way.

3.1 Markov chain model for spectrum mobility

The method of DTMC to capture spectrum mobility is defined by its state, transfer probability, and steady probability. In what follows, we assume that the arrival probability and departure probability for MBS users are λ_{a} and λ_{d}, respectively.

1. State

Assuming that there are M time slots occupied by MBS users on the channel, we use $\psi=\{\psi(u)=0 \text{ or } 1, u=1, 2, \ldots, M\}$ to represent the occupancy state of all MBS users, where $\psi(u)=0$ means that the MBS user is on the channel while $\psi(u)=1$ means it is absent. Then $\phi(i)=\sum_{u=1}^{M}\psi(u)=i$ $(0\le i\le D)$ denotes that there are i MBS users in the frame and D is the number of time slots.

2. Transfer probability

Here MBS users arrive and depart in a Poisson way; meanwhile, once one MBS user arrives, a single time slot of consecutive frames will be occupied for an exponentially distributed time period until it leaves. The probability of k ($k\le i$) MBS users' arrival during the frame is given by

$$p_{\mathrm{A}}(k)=p\{N_{\mathrm{A}}=k\}=\frac{(\lambda_{\mathrm{a}}T_{\mathrm{frame}})^k}{k!}\mathrm{e}^{-\lambda_{\mathrm{a}}T_{\mathrm{frame}}}, \tag{5}$$

where N_{A} is the number of MBS users which arrive at the channel during the frame and $T_{\mathrm{frame}}=D\times T_{\mathrm{slot}}$ means the total time of the frame.

Since both the arrival and departure for MBS users follow a Poisson way, the probability that at least one MBS user leaves is

$$p_{\mathrm{D}}=1-p_{\mathrm{D}}(0)=1-\mathrm{e}^{-\lambda_{\mathrm{d}}T_{\mathrm{frame}}}, \tag{6}$$

where $p_{\mathrm{D}}(0)$ means there is no MBS user leaving the channel. Then the probability of l departures out of i MBS users during the frame is given by

$$\begin{aligned}p_{\mathrm{D}}(i,l)&=p\{N_{\mathrm{D}}=l\}\\&=\binom{i}{l}(1-\mathrm{e}^{-\lambda_{\mathrm{d}}T_{\mathrm{frame}}})^l(\mathrm{e}^{-\lambda_{\mathrm{d}}T_{\mathrm{frame}}})^{i-l},\end{aligned} \tag{7}$$

where N_D is the number of MBS users leaving the channel during the frame.

Therefore, in state $\phi(i)$, the probability of k MBS users' arrival with l users' departure is expressed as

$$A(i,k,l)=\begin{cases}p_A(k), & i-l+k<D,\\ 1-\sum_{d=0}^{k-1}p_A(d), & i-l+k=D.\end{cases} \tag{8}$$

Correspondingly, the probability of l departures in state $\phi(i)$ is

$$D(i,k,l)=p_D(i,l). \tag{9}$$

The transition probability matrix $\boldsymbol{P}$ can be derived by calculating all the state transform probabilities p_{ij} from $\phi(i)$ to $\phi(i+H)$. An element of the matrix is derived as

$$\begin{aligned}p_{ij}&=p_{i+H,i}=p((i+H)|i)\\&=\sum_{k=\max(-H,0)}^{i}A(i,H+k,k)D(i,H+k,k)\\&\quad(0\le i\le D,-i\le H\le D).\end{aligned} \tag{10}$$

3. Steady probability $\pi(i)$

Constructing the steady state probability $\pi(i)$ (i=0, 1, …, D) as the elements of matrix $\boldsymbol{\Pi}$=[π(0), π(1), …, $\pi(D)$], we are able to obtain $\pi(i)$ by finding the solution with respect to the following condition equation:

$$\boldsymbol{\Pi}=\boldsymbol{\Pi}\cdot\boldsymbol{P}. \tag{11}$$

4. Ideal MBS and SBS users

For the case of ideal sensing, the average number of ideal MBS users during the frame can be calculated by accumulating all the possible states:

$$N_p=\sum_{i=0}^{D}i\cdot\pi(i). \tag{12}$$

Therefore, the average number of ideal SBS users is as follows:

$$N_s=D-N_p. \tag{13}$$

5. Considering the case of miss-detection

For the case of non-ideal sensing, the number of MBS users on the channel needs to be modified. Firstly, we take the miss-detection error into consideration. In what follows, the modified metrics from the perspective of SBS users are discussed. Assuming that events of miss-detection and false-alarm are independent, we can derive the modifying factor by considering all the situations:

$$\alpha(i,m)=\begin{cases}\sum_{m=0}^{i}\binom{i}{m}p_{md}^{m}(1-p_{md})^{i-m}, & 0\le i\le D,\ 0\le m\le i,\\ 0, & 0\le i\le D,\ i<m\le D,\end{cases} \tag{14}$$

where p_{md} is the miss-detection probability.

Thus, the number of time slots with miss-detection in state $\phi(i)$ is redefined as

$$N_{Sh}=\sum_{m=0}^{D}\sum_{i=0}^{D}\alpha(i,m)m\pi(i), \tag{15}$$

while the number of time slots occupied by pure MBS users is refreshed as

$$N_M=N_p-N_{Sh}. \tag{16}$$

6. Considering the case of false-alarm

Similarly, the total probability modifying factor due to the false-alarm error is given by

$$\beta(i,k)=\begin{cases}\sum_{k=0}^{D-i}\binom{D-i}{k}p_{fa}^{k}(1-p_{fa})^{D-i-k}, & 0\le i\le D,\ 0\le k\le D-i,\\ 0, & 0\le i\le D,\ D-i<k\le D,\end{cases} \tag{17}$$

where p_{fa} is the false-alarm probability.

The number of free time slots in state $\phi(i)$ is

$$N_{Free}=\sum_{k=0}^{D}\sum_{i=0}^{D}\beta(i,k)k\pi(i). \tag{18}$$

After defining the interfering time slots with shared and free slots with respect to MP and FP, the number of time slots with pure SBS users is concluded as

$$N_{\mathrm{F}} = D - N_{\mathrm{M}} - N_{\mathrm{Sh}} - N_{\mathrm{Free}} = N_{\mathrm{s}} - N_{\mathrm{Free}}. \quad (19)$$

To make the ideal and non-ideal cases clear, the distribution of time slots with or without sensing errors is illustrated in Fig. 2.

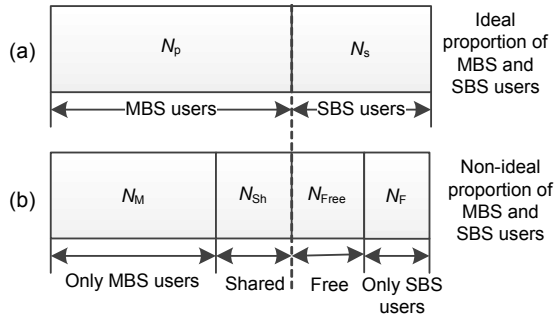

Fig. 2 Time slots distribution with (a) or without (b) miss-detection and false-alarm errors

3.2 Approximating capacity of CHN with HPPP assumption

In this paper, assuming that interference is captured by the density of base stations, we consider an integral way to derive the interference. The idea derives from a 'fluid model' (Kelif and Alman, 2005; Khawam *et al.*, 2007) which uses the integral of the density of BSs in the whole network to calculate the capacity. In HPPP models, BSs are randomly distributed in a series of concentric circles, and the areas of the annuluses between two adjacent concentric circles follow Poisson distribution along the radial direction from the center (Fig. 3).

Lemma 1 In the HPPP model as defined, the probability density function (PDF) of distance r can be given by

$$f(r) = 2\lambda\pi r\mathrm{e}^{-\lambda\pi r^2}. \quad (20)$$

Proof According to the definition of the Poisson point process, we have

$$g(r) = \mathrm{e}^{-\lambda\pi r^2}, \quad (21)$$

where $g(r)$ is the cumulative density function (CDF) of the event that no BS is closer than r.

In the HPPP model, there is only one BS on one single circle. Therefore, the CDF of distance r can be expressed as

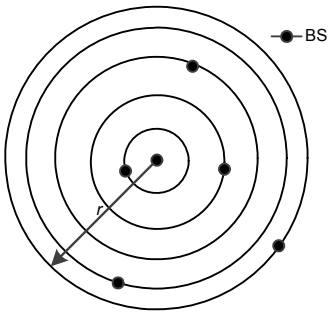

Fig. 3 The distribution sketch of the homogeneous Poisson point process (HPPP)

$$F(r) = 1 - g(r) = 1 - \mathrm{e}^{-\lambda\pi r^2}. \quad (22)$$

Taking the derivative of r with respect to $F(r)$, we can obtain the PDF of distance r as given by Eq. (20). Namely, the probability that an interference BS occurs in the distance of r from the user is $f(r)$.

As to the channel model, we consider only power loss propagation for short. Define the path loss model as $L(r)=r^{\alpha}$, where α is the decaying rate of fast fading. Taking the integral in the coverage of interfering base stations, we can obtain the interference for MBS and SBS users, respectively. The following analysis uses the notion of typicality of HPPP, which is made precise using Palm theory (Stoyan *et al.*, 1995). In brief, Palm theory shows that every point in HPPP enjoys the same status and the whole distribution appears to be the same when it is observed at an arbitrary location.

For the case of ideal sensing (Fig. 2a), only co-tier interference exists. Therefore, there are two kinds of interference categorized for different tiers:

1. When the channel is occupied by MBS users, for a specific MBS user, the interference from other MBSs is given by

$$I_{\mathrm{M},m} = \int_0^{2\pi}\int_x^R p_{\mathrm{M}}\lambda_{\mathrm{M}} 2\pi r\mathrm{e}^{-\lambda_{\mathrm{M}}\pi r^2} r^{\alpha}\mathrm{d}r\mathrm{d}\theta. \quad (23)$$

2. Similarly, when the channel is occupied by SBS users, the interference from other SBSs is as follows:

$$I_{\mathrm{F},f} = \int_0^{2\pi}\int_x^R p_{\mathrm{F}}\lambda_{\mathrm{F}} 2\pi r\mathrm{e}^{-\lambda_{\mathrm{F}}\pi r^2} r^{\alpha}\mathrm{d}r\mathrm{d}\theta, \quad (24)$$

where x is the distance between the BS and its serving user, which satisfies the conditions $R>>x$ and $R>>0$.

For the case of non-ideal sensing (Fig. 2b), there are four different cases. In particular, when the channel is occupied by both MBS users and SBS users in shared time slots, there is also cross-tier interference except for co-tier interference.

1. When the time slots are free, there is no interference.

2. When the channel is occupied by MBS users, the interference is the same as Eq. (23).

3. When the channel is occupied by SBS users, the interference can be expressed by Eq. (24).

4. When there are both MBS and SBS users on the channel, for a specific MBS user, the interference from all the SBSs is as follows:

$$I_{\mathrm{F},m}=\int_0^{2\pi}\int_0^R p_{\mathrm{F}}\lambda_{\mathrm{F}}2\pi r\mathrm{e}^{-\lambda_{\mathrm{F}}\pi r^2}r^{\alpha}\mathrm{d}r\mathrm{d}\theta \approx\frac{2\pi p_{\mathrm{F}}\Gamma(\alpha/2+1)}{(\pi\lambda_{\mathrm{F}})^{\alpha/2}}, \tag{25}$$

where $\Gamma(x)=\int_0^{+\infty}t^{x-t}\mathrm{e}^{-t}\mathrm{d}t$.

For a specific MBS user, the interference from all the MBSs is derived by

$$I_{\mathrm{M},f}=\int_0^{2\pi}\int_0^R p_{\mathrm{M}}\lambda_{\mathrm{M}}2\pi r\mathrm{e}^{-\lambda_{\mathrm{M}}\pi r^2}r^{\alpha}\mathrm{d}r\mathrm{d}\theta \approx\frac{2\pi p_{\mathrm{M}}\Gamma(\alpha/2+1)}{(\pi\lambda_{\mathrm{M}})^{\alpha/2}}. \tag{26}$$

Remark 1 Due to the assumption of $R>>0$, Eqs. (25) and (26) can be approximated as Gamma functions. However, Eqs. (23) and (24) cannot be written in a similar way since the lower limitation is starting from x.

To conclude, the whole network capacity for the ideal sensing case can be expressed as

$$\begin{aligned}C&=C_{\mathrm{M}}+C_{\mathrm{F}}\\&=\frac{W\eta}{D}\left[N_{\mathrm{p}}\sum_{m=1}^{X}\log_2(1+\mathrm{SINR}_m)+N_{\mathrm{s}}\sum_{f=1}^{Y}\log_2(1+\mathrm{SINR}_f)\right],\end{aligned} \tag{27}$$

where W is the bandwidth of the channel, $\eta=1-T_{\mathrm{s}}/T_{\mathrm{slot}}$ is the sensing efficiency, and C_{M} and C_{F} represent the capacities of the macro cell and small cell in an ideal sensing case, respectively.

When there exist sensing errors, the capacity of the whole network is modified by

$$\begin{aligned}\overline{C}&=\overline{C}_{\mathrm{M}}+\overline{C}_{\mathrm{F}}\\&=\frac{W\eta}{D}\left[N_{\mathrm{M}}\sum_{m=1}^{X}\log_2(1+\mathrm{SINR}_m)+N_{\mathrm{F}}\sum_{f=1}^{Y}\log_2(1+\mathrm{SINR}_f)\right.\\&\quad\left.+N_{\mathrm{Sh}}\left(\sum_{m=1}^{X}\log_2(1+\overline{\mathrm{SINR}}_m)+\sum_{f=1}^{Y}\log_2(1+\overline{\mathrm{SINR}}_f)\right)\right],\end{aligned} \tag{28}$$

where $\overline{C}_{\mathrm{M}}$ and $\overline{C}_{\mathrm{F}}$ are the capacities of the macro cell and small cell in the non-ideal sensing case, respectively.

4 Simulation results and analysis

To verify the proposed capacity expression, we present several numerical metrics and give relative analysis in this section. In the simulation, we assume that the MBSs, SBSs, and users in the two-tier CHN are distributed within a circle of radius 500 m, following an HPPP way with densities 0.00004, 0.0008, and 0.0016 m^{-2}, respectively. The remaining simulation parameters are listed in Table 1, and an illustration of the two-tier heterogeneous network is shown in Fig. 4. In what follows, we present the comparison of the capacity of the uniform model and HPPP model as well as the results derived by integral and sum

Table 1 Simulation parameters

Parameter	Definition	Value
P_{M}	Transmit power of MBS	20 W
P_{F}	Transmit power of SBS	0.1 W
P_{Noise}	Power of noise	1 W
W	Physical bandwidth	1 Hz
α	Decaying rate of fast fading	3
D	Number of slots in a frame	20
T_{slot}	Period of a time slot	0.577 ms
T_{s}	Period of sensing time	25 μs
λ_{a}	AP of the MBS users	0.1–0.9 (0.8*)
λ_{d}	DP of the MBS users	0.1–0.9 (0.5*)
p_{md}	Miss-detection probability	0–0.99 (0.01*)
p_{fa}	False-alarm probability	0–0.99 (0.73*)

* Default value

methods. Furthermore, the effect of the arrival probability (AP) and departure probability (DP) is analyzed, while the effect of ideal and non-ideal sensing on capacity is presented.

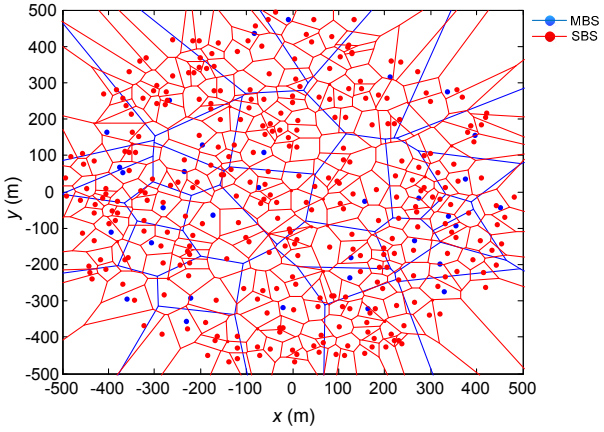

Fig. 4 Two-tier heterogeneous network (λ_M=0.00004 m^{-2}, λ_F=0.0008 m^{-2}, R=500 m)
References to color refer to the online version of this figure

4.1 Capacity comparison of the proposed method

Before presenting the results of the proposed statistical methods for CHNs capacity, we first compare the capacity of different models (Fig. 5), i.e., the HPPP model and uniform model (where MBSs and SBSs are uniformly distributed). It can be observed that the capacity in the two models keeps growing with the density of SBSs, while the uniform model reaches a higher network capacity than the HPPP model. This is because the likelihood of a dominant interferer is higher for the HPPP model and the same results can be found in ElSawy *et al.* (2013b). Also, we can observe that the capacities of the two models become close when the density of SBSs increases. Thus, the HPPP model provides a lower bound on capacity than traditional uniform models; meanwhile, at a high density of the network, regularity or irregularity matters little.

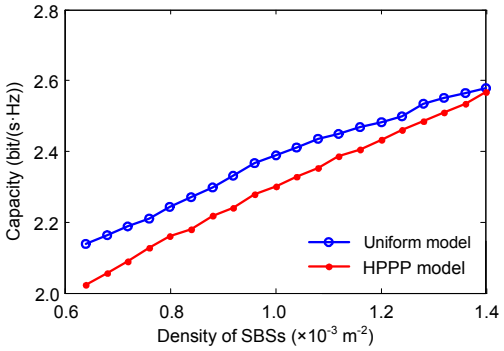

Fig. 5 Capacity comparison between the uniform model and HPPP model by the integral method (λ_M=0.00004 m^{-2}, λ_F=0.0008 m^{-2}, R=500 m)

We simulate the capacity of the network derived by the integral method and sum method in the HPPP model (Fig. 6). It can be figured out that the integral method has a lower capacity than the sum method. The reason lies in the fact that the integral method calculates interference from a continuous aspect while the sum method supposes that the base stations are distributed in a discrete way. Thereby, the integral method aggregates a higher interference resulting in a lower capacity. Also, as the density of SBSs increases, the gap between these two methods becomes smaller (when the density of SBSs increases from 0.00063 to 0.0014 m^{-2}, the gap decreases from 12% to 1%). This is because a continuous distribution of base stations approaches the discrete distribution at the high density of SBSs.

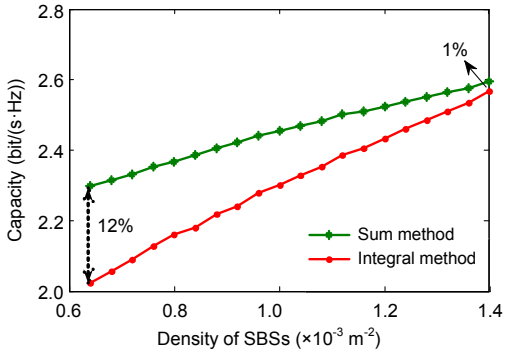

Fig. 6 Comparison between the integral method and sum method in the HPPP model (λ_M=0.00004 m^{-2}, λ_F=0.0008 m^{-2}, R=500 m)

4.2 Effect of the mobility of MBS users

In this subsection, we discuss the capacity of the network under different APs and DPs to analyze the effect of the mobility of MBS users on the capacity of the network (Figs. 7–10).

Fig. 7 illustrates the network capacity under different departure probabilities with the increase in AP of MBS users. It can be observed that the network capacity keeps growing with the increase in AP of MBS users when DP is 0.2, 0.5, and 0.9, respectively.

When DP is 0.1, however, the network capacity exhibits a slight decline. Actually, at low DP values, the high AP of MBS users impacts the capacity by deteriorating the interference, which results in a lower capacity (when AP goes from 0 to 1, the capacity decreases by 5%). Conversely, in the case of high DP, there are more time slots occupied by MBS users with the increase in AP of MBS users, which results in a higher capacity.

The capacity under different APs with a variance in DP of MBS users is shown in Fig. 8. We can observe that the curves flare up at low DP but show a decline when DP is over certain values. Meanwhile, there is an optimal DP for each curve, which can be inferred from Eq. (7). The reason is that the whole capacity includes macro-cell capacity and small-cell capacity, and macro-cell capacity has a similar tendency to the whole capacity (Figs. 9 and 10). It can be observed that the macro-cell capacity curve has the same tendency as the whole capacity curve while the small-cell capacity curve acts conversely. In fact, in the case of low DP, more users can connect to MBSs rather than SBSs with the increasing DP, which leads to a higher macro-cell capacity. However, when DP goes higher, the total number of MBS users in the network becomes less, which results in a lower macro-cell capacity. Opposite results can be derived for the capacity SBS network since MBS and SBS users share the same frequency during each frame in the overlay fashion.

4.3 Effect of sensing errors

Capacity with or without sensing errors is considered in this part, i.e., ideal case and non-ideal case, and the comparison is illustrated in Figs. 11 and 12. Fig. 11 describes the ideal and non-ideal cases with various APs. Considering DP of 0.1 and 0.2, the curves of the ideal case are above those of the non-ideal one. This verifies that sensing errors reduce the system capacity to a certain degree. Similar conclusions can be drawn from Fig. 12. This is because, in the case of ideal sensing, there are more MBS users

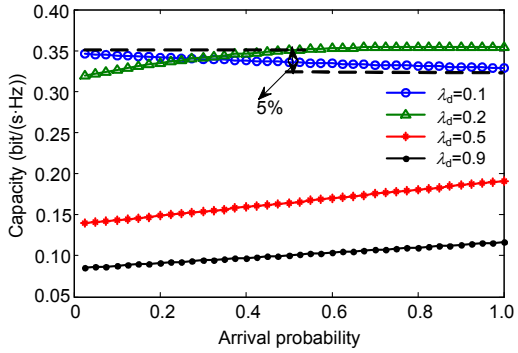

Fig. 7 Capacities under different arrival probabilities (p_{md}=0.01, p_{fa}=0.73)

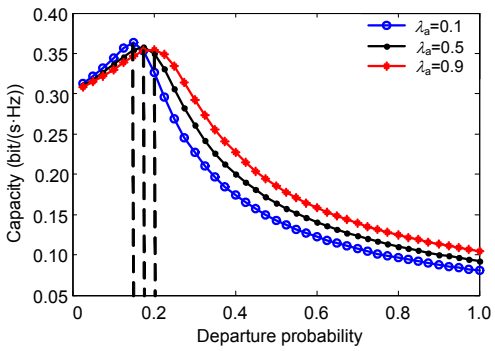

Fig. 8 Capacities under different departure probabilities (p_{md}=0.01, p_{fa}=0.73)

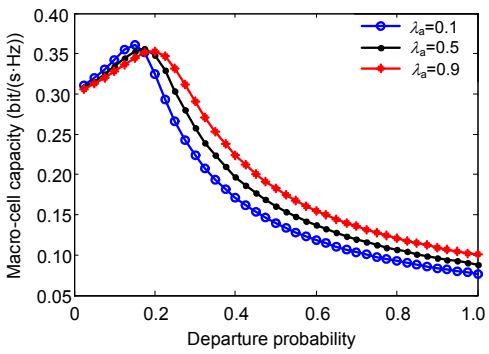

Fig. 9 Macro-cell capacities under different departure probabilities (p_{md}=0.01, p_{fa}=0.73)

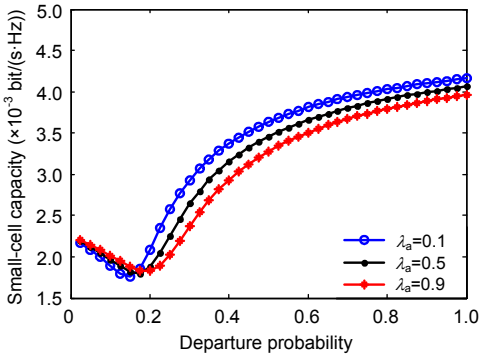

Fig. 10 Small-cell capacities under different departure probabilities (p_{md}=0.01, p_{fa}=0.73)

and fewer free users on the channel, which brings a higher capacity. Generally speaking, high sensing accuracy helps improve the network capacity.

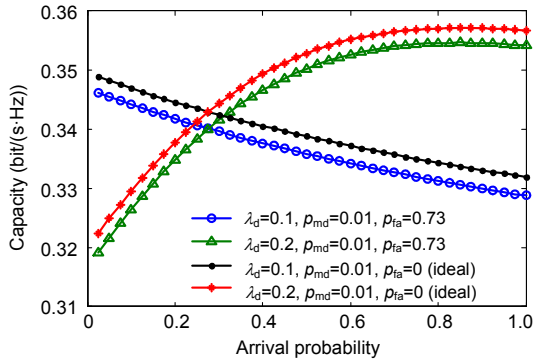

Fig. 11 Capacities under different arrival probabilities for ideal and non-ideal cases

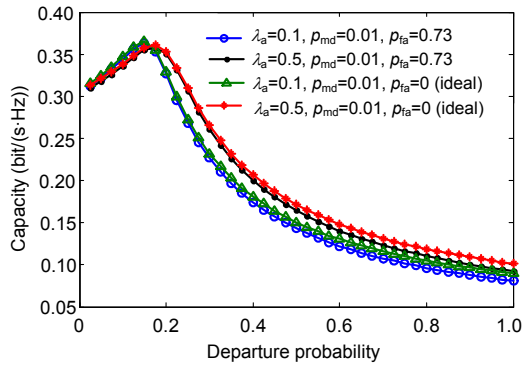

Fig. 12 Capacities under different departure probabilities for ideal and non-ideal cases

5 Conclusions and future work

In this paper, we have derived the network capacity by stochastic geometric methods in a two-tier CHN model. DTMC has been employed to capture the spectrum mobility, while an integral method has been proposed to approximate the interference under different sensing results. Based on the HPPP network model, simulation results have been illustrated to show that the proposed method turns out to be a simple and efficient way to calculate capacity in CHNs. Moreover, we have analyzed the effect of arrival and departure probabilities on CHN capacity. It has been shown that there is an optimal DP for each AP. Finally, comparison has been made between the capacities of ideal and non-ideal cases, and the results verify that the non-ideal case has a higher capacity. In future work we plan to focus on capacity analysis for hyper-dense heterogeneous and small-cell networks.

References

Akoum, S., Zwingelstein-Colin, M., Heath, R.W., *et al.*, 2010. Cognitive cooperation for the downlink of frequency reuse small cells. Proc. 2nd Int. Workshop on Cognitive Information Processing, p.111-115. [doi:10.1109/CIP.2010.5604251]

Akoum, S., Kountouris, M., Heath, R.W., 2011. On imperfect CSI for the downlink of a two-tier network. Proc. IEEE Int. Symp. on Information Theory, p.553-557. [doi:10.1109/ISIT.2011.6034189]

Andrews, J.G., Baccelli, F., Ganti, R.K., 2011. A tractable approach to coverage and rate in cellular networks. *IEEE Trans. Commun.*, **59**(11):3122-3134. [doi:10.1109/TCOMM.2011.100411.100541]

Bennis, M., Perlaza, S.M., Blasco, P., *et al.*, 2013. Self-organization in small cell networks: a reinforcement learning approach. *IEEE Trans. Wirel. Commun.*, **12**(7):3202-3212. [doi:10.1109/TWC.2013.060513.120959]

Dhillon, H.S., Ganti, R.K., Baccelli, F., *et al.*, 2012a. Modeling and analysis of *K*-tier downlink heterogeneous cellular networks. *IEEE J. Sel. Area Commun.*, **30**(3):550-560. [doi:10.1109/JSAC.2012.120405]

Dhillon, H.S., Novlan, T.D., Andrews, J.G., 2012b. Coverage probability of uplink cellular networks. Proc. IEEE Global Communications Conf., p.2179-2184. [doi:10.1109/GLOCOM.2012.6503438]

ElSawy, H., Hossian, E., 2013. Two-tier HetNets with cognitive femtocells: downlink performance modeling and analysis in a multichannel environment. *IEEE Trans. Mob. Comput.*, **13**(3):649-663. [doi:10.1109/TMC.2013.36]

ElSawy, H., Hossain, E., Kim, D.I., 2013a. HetNets with cognitive small cells: user offloading and distributed channel access techniques. *IEEE Commun. Mag.*, **51**(6):28-36. [doi:10.1109/MCOM.2013.6525592]

ElSawy, H., Hossain, E., Haenggi, M., 2013b. Stochastic geometry for modeling, analysis, and design of multi-tier and cognitive cellular wireless networks: a survey. *IEEE Commun. Surv. Tutor.*, **15**(3):996-1019. [doi:10.1109/SURV.2013.052213.00000]

Fehske, A.J., Viering, I., Voigt, J., *et al.*, 2014. Small-cell self-organizing wireless networks. *Proc. IEEE*, **102**(3):334-350. [doi:10.1109/JPROC.2014.2301595]

Gelabert, X., Sallent, O., Pérez-Romero, J., *et al.*, 2010. Spectrum sharing in cognitive radio networks with imperfect sensing: a discrete-time Markov model. *Comput. Netw.*, **54**(14):2519-2536. [doi:10.1016/j.comnet.2010.04.005]

Heath, R.W., Kountouris, M., Bai, T., 2013. Modeling heterogeneous network interference using Poisson point processes. *IEEE Trans. Signal Process.*, **61**(16):4114-4126. [doi:10.1109/TSP.2013.2262679]

Huang, Y.C., Ko, K.T., Huang, Q., *et al.*, 2011. An efficient method for performance evaluation of femto-macro overlay systems. Proc. IEEE Int. Conf. on communications, p.1-6. [doi:10.1109/icc.2011.5962706]

Hwang, I., Song, B., Soliman, S.S., 2013. A holistic view on hyper-dense heterogeneous and small cell networks. *IEEE Commun. Mag.*, **51**(6):20-27. [doi:10.1109/MCOM.2013.6525591]

Kelif, J.M., Alman, E., 2005. Downlink fluid model of CDMA networks. Proc. IEEE 61st Vehicular Technology Conf., p.2264-2268. [doi:10.1109/VETECS.2005.1543738]

Khawam, K., Samhat, A.E., Ibrahim, M., *et al.*, 2007. Fluid model for wireless adhoc networks. Proc. IEEE 18th Int. Symp. on Personal, Indoor and Mobile Radio Communications, p.1-5. [doi:10.1109/PIMRC.2007.4394499]

Khoshkholgh, M., Navaie, K., Yanikomeroglu, H., 2013. Outage performance of the primary service in spectrum sharing networks. *IEEE Trans. Mob. Comput.*, **12**(10):1955-1971. [doi:10.1109/TMC.2012.156]

Madhusudhanan, P., Restrepo, J.G., Liu, Y., *et al.*, 2012. Heterogeneous cellular network performance analysis under open and closed access. Proc. IEEE Globecom Workshops, p.563-568. [doi:10.1109/GLOCOMW.2012.6477635]

Meerja, K.A., Ho, P.H., Wu, B., 2011. A novel approach for co-channel interference mitigation in femtocell networks. Proc. IEEE Global Telecommunications Conf., p.1-6. [doi:10.1109/GLOCOM.2011.6133956]

Nakamura, T., Nagata, S., Benjebbour, A., *et al.*, 2013. Trends in small cell enhancements in LTE advanced. *IEEE Commun. Mag.*, **51**(2):98-105. [doi:10.1109/MCOM.2013.6461192]

Stoyan, D., Kendall, W.S., Mecke, J., 1995. Stochastic Geometry and Its Applications (2nd Ed.). John Wiley & Sons, Chichester.